Preparation and Properties of $Ru_2(DtolF)_4Cl$: A Surprising Electronic Structure Change Compared to $Ru_2(DtolF)_4$ (DtolF = [(*p*-tol)NCHN(*p*-tol)]$^-$)

F. Albert Cotton* and Tong Ren

Department of Chemistry, Texas A&M University, College Station, Texas 77843-3255

Received November 30, 1994[⊗]

Through the reaction between $Ru_2(OAc)_4Cl$ and molten HDtolF (di-*p*-tolylformamidine), $Ru_2(DtolF)_4Cl$ (**1**) was isolated as a crystalline material in 75% yield. The green complex crystallizes as $Ru_2(DtolF)_4Cl{\cdot}C_6H_{14}$ in the tetragonal space group *P4/ncc*, with a = 16.400 (3) Å, c = 22.042(3) Å, V = 5928 (2) Å^3, and Z = 4. The Ru−Ru distance was found to be 2.370(2) Å, which is *ca.* 0.1 Å shorter than that in the known $Ru_2(DtolF)_4$. On the basis of the temperature dependence of the effective magnetic moment, the compound is best described as a $S = {}^3/_2$ system which undergoes zero-field splitting with D = 49.5 cm^{-1}. A $\sigma^2\pi^4\delta^2\pi^{*2}\delta^*$ configuration is suggested for the ground state. Reversible oxidation occurs at 493 mV (Ag/AgCl) in the cyclic voltammogram, suggesting the accessibility of a $Ru_2(DtolF)_4^{2+}$ species.

Introduction

We recently reported the compound $Ru_2(DtolF)_4$, a compound containing the multiply bonded Ru_2^{4+} core (with Ru−Ru distance of 2.474(1) Å and no unpaired electrons) supported by the four bridging ligands [(*p*-tol)NCHN(*p*-tol)]$^-$, which we abbreviate[1] DtolF$^-$. This remarkable molecule has the longest Ru−Ru distance ever reported in this general class of compounds, and its diamagnetism is also notable. Both of these facts can be accounted for when it is realized that, as shown by SCF−Xα−SW calculations,[2,3] the RNXNR$^-$ type ligands with X = N or CR′ interact with M_2^{n+} cores in such a way as to raise the energy of the δ^* orbital above that of the π^* orbital. Thus, for $Ru_2(DtolF)_4$ as well as for the previously reported $Ru_2[(p\text{-tol})NNN(p\text{-tol})]_4$[4] and $Ru_2(PhNNNPh)_4$[5] molecules, the electron configuration is $\sigma^2\pi^4\delta^2\pi^{*4}$. The large number of π^* electrons accounts for the Ru−Ru distances in all three cases.

Two previous attempts were made to determine the consequences of the one-electron oxidation of the $Ru_2(RNXNR)_4$ compound. One led to the isolation[6] of $Ru_2(PhNNNPh)_4OPF_4$ in which the Ru−Ru bond distance, 2.385(2) Å, was not significantly (in a chemical sense) shorter than that[5] in $Ru_2(PhNNNPh)_4$, 2.399(1) Å. Similarly, the change[5] in Ru−Ru distance on going from $\{Ru_2[(p\text{-tol})NNN(p\text{-tol})]_4(CH_3CN)\}$ to $\{Ru_2[(p\text{-tol})NNN(p\text{-tol})]_4(CH_3CN)\}BF_4$, 2.407(1) to 2.373(1) Å, while larger, is also rather small. Three factors should influence the net change in bond length: (1) Loss of a π^* electron might be expected, by itself, to favor a significant shortening of the bond, by perhaps 0.10 Å. (2) Offsetting this would be the fact that the increase in charge in the dimetal core, from Ru_2^{4+} to Ru_2^{5+}, would tend to weaken all the bonding interactions. (3) The tighter binding of axial ligands to the Ru_2^{5+} core would also tend to reduce the σ Ru−Ru bond strength. The observation that only very small decreases in the Ru−Ru distance occur in the cases just cited could thus be explained, if factors 2 and 3 nullify much of the expected effect of losing a π^* electron.

In an effort to explore the behavior of such species better, we considered it worthwhile to study the analogous $Ru_2(DtolF)_4$/$Ru_2(DtolF)_4^+$ system. Direct oxidation of $Ru_2(DtolF)_4$ led only to an intractable product, but we have been able to obtain one oxidation product, $Ru_2(DtolF)_4Cl$, by an indirect route. Here we have found a much greater decrease of 0.106(2) Å. However, a magnetic susceptibility study shows that $Ru_2(DtolF)_4$ and $Ru_2(DtolF)_4Cl$ are **not** related by simple removal of one π^* electron (accompanied by attachment of axial Cl$^-$) but that a more extensive change in the electronic structure takes place, such that $Ru_2(DtolF)_4Cl$ evidently has a $\sigma^2\pi^4\delta^2\pi^{*2}\delta^*$ configuration.

Experimental Section

The synthesis was carried out in an argon atmosphere using standard Schlenkware. $Ru_2(OAc)_4Cl$ and di-*p*-tolylformamidine were obtained as previously described.[2] All solvents used were freshly distilled over suitable drying reagents under N_2. The UV/vis (800−250 nm) spectrum was recorded on a Cary-17 spectrometer at ambient temperature using quartz cells. The cyclic voltammogram was recorded on a BAS 100 electrochemical analyzer in 0.1 M $(n\text{-Bu})_4NBF_4$ solution (CH_2Cl_2) with a Pt working electrode and a Ag/AgCl reference electrode. Ferrocene was oxidized at 576 mV under the experimental conditions. The magnetic susceptibility was measured at the University of South Carolina on a superconducting quantum interference device (SQUID) by Prof. T. Datta and Dr. J. Amirzadek. Microanalysis was performed by Galbraith Laboratories, Inc., Knoxville, TN.

Preparation of $Ru_2(DtolF)_4Cl$. $Ru_2(OAc)_4Cl$ (0.48 g, 1.0 mmol) and HDtolF (2.70 g, 12.0 mmol) were heated under argon at *ca.* 155 °C for 3 h. A large amount of acetic acid was evolved while the initially red molten suspension became black. The excess ligand was removed by vacuum sublimation at 125 °C. The dark residue was extracted with 2 × 10 mL of benzene to yield a bright red solution which was shown to contain the known $Ru_2(DtolF)_4$ by the UV/vis spectrum.[2] A large amount of dark green microcrystalline material was left on the frit. Vacuum distillation of benzene from the red solution afforded 0.17 g of $Ru_2(DtolF)_4$ (17% based on $Ru_2(OAc)_4Cl$). The dark green solid was again treated with 12 mmol of HDtolF at 155 °C for 2 h to ensure complete displacement of the acetate ligands. A small amount of acetic acid was indeed observed to condense on the cold finger placed above the reactants. The molten mixture was allowed to cool to *ca.* 80 °C, and 20 mL of benzene was added with vigorous stirring to form a suspension. After 1 h at room temperature the dark green crystalline precipitate was collected by filtration and further washed with a copious

[⊗] Abstract published in *Advance ACS Abstracts,* June 1, 1995.

(1) The DtolF notation belongs to a new systematic scheme: Cotton, F. A.; Daniels, L. M.; Maloney, D. J.; Matonic, J. H.; Murillo, C. A. *Polyhedron* **1994**, *13*, 815. The previously used code was DFM.
(2) Cotton, F. A.; Ren, T. *Inorg. Chem.* **1991**, *30*, 3675.
(3) Cotton, F. A.; Feng, X. *Inorg. Chem.* **1989**, *28*, 1180.
(4) Cotton, F. A.; Matusz, M. *J. Am. Chem. Soc.* **1988**, *110*, 5761.
(5) Cotton, F. A.; Falvello, L. R.; Ren, T.; Vidyasagar, K. *Inorg. Chim. Acta* **1992**, *194*, 163.
(6) Cotton, F. A.; Matusz, M. *Chimia* **1989**, *43*, 167.

0020-1669/95/1334-3190$09.00/0

Table 1. Data Collection and Refinement Parameters for $Ru_2(DtolF)_4Cl{\cdot}C_6H_{14}$

formula	$Ru_2ClN_8C_{66}H_{74}$
fw	1217.0
a, Å	16.400(3)
c, Å	22.042(3)
V, Å^3	5928(2)
Z	4
space group	*P4/ncc* (No. 130)
T, °C	20
radiation monochromated in incident beam: λ(Cu Kα), Å	1.541 84
d_{calcd}, g/cm^3	1.363
μ(Cu Kα), cm^{-1}	50.7
transm factors: max, min	1.00, 0.75
R^a	0.055
$R_w{}^b$	0.063
quality-of-fit indicator^c	2.16

^{a} $R = \sum||F_o| - |F_c||/\sum|F_o|$. ^{b} $R_w = [\sum w(|F_o| - |F_c|)^2/\sum w|F_o|^2]^{1/2}$; $w = 1/\sigma^2(|F_o|)$. ^{c} Quality-of-fit = $[\sum w(F_o - F_c)^2/(N_{observns} - N_{params})]^{1/2}$.

amount of benzene to remove the free ligand. There was no detectable amount of $Ru_2(DtolF)_4$ in the filtrate this time. Yield: 75%. A large quantity of column-like crystals was obtained by layering of a CH_2Cl_2 solution with hexane. Anal. Calcd (found): C, 63.7 (64.1); H, 5.4 (5.5); N, 10.0 (9.3). UV/vis/near-IR (CH_2Cl_2) [λ, nm (ϵ, M^{-1} cm^{-1})]: 679 (2180), 469 (5420).

X-ray Crystallography. A dark plate of dimensions 0.35 × 0.15 × 0.08 mm^3 was wedged in a Lindemann capillary together with mineral oil saturated with mother liquor. A tetragonal cell was derived by the initial indexing of 16 reflections in the range 38° ≤ 2θ ≤ 49°, and the Laue symmetry (*4/mmm*) was confirmed by normal-beam oscillation photographs. The space group was uniquely determined as *P4/ncc* (No. 130) from the systematic absences. Diffraction data were collected on a Rigaku AFC5R diffractometer using monochromated Cu Kα radiation. The data set was corrected for Lorentz, polarization, and decay (overall −1.0%) effects. An empirical absorption correction based on the ψ-scan method was also applied to the data.[7]

A Patterson map revealed all the peaks corresponding to the whole $Ru_2(DtolF)_4Cl$ molecule with both ruthenium atoms and the axial chlorine atom sitting on the crystallographic 4-fold axis. All these atoms were refined with anisotropic thermal parameters to low residuals. A difference Fourier map thereafter revealed a number of peaks about a site of *2/m* symmetry, corresponding to a hexane molecule, which is also disordered by the 2-fold axis on which two of the carbon atoms reside. The solvent molecule did not refine freely very well in SDP and was refined to convergence with the carbon−carbon bond length restraint in SHELX-76. The final figures of merit are collected in Table 1, while the fractional coordinates are listed in Table 2.

Results and Discussion

The synthesis of $Ru_2(DtolF)_4Cl$ employed the same general approach that was previously used for some diruthenium hydroxypyridinate compounds,[8,9] as well as for $Os_2(DtolF)_4Cl_2$.[10] The overall process can be summarized as follows:

$$Ru_2(OAc)_4Cl + HDtolF \rightarrow Ru_2(DtolF)_4Cl\ (ca.\ 80\%) + Ru_2(DtolF)_4\ (\leq 20\%) \quad (1)$$

While the partial reduction was not anticipated, it can be attributed to the action of the great excess of HDtolF. It presumably occurs in an early stage only, when the bulky HDtolF molecule still has access to the Ru−Cl unit. This access is presumably blocked after most of the acetate groups have been replaced by $DtolF^-$ ions, since no $Ru_2(DtolF)_4$ was formed in the repeated fusion that was done to remove any small amounts of acetate remaining after the first one.

Table 2. Positional Parameters and Their Estimated Standard Deviations for $Ru_2(DtolF)_4Cl{\cdot}C_6H_{14}$[a]

atom	x	y	z	B, Å^2
Ru(1)	0.250	0.250	0.14301(5)	3.52(3)
Ru(2)	0.250	0.250	0.25054(5)	3.56(3)
Cl	0.250	0.250	0.3600(2)	6.4(1)
N(1)	0.2983(4)	0.1360(4)	0.1431(3)	3.7(2)
N(2)	0.3287(4)	0.1499(4)	0.2451(3)	4.0(2)
C(1)	0.3343(5)	0.1101(5)	0.1936(3)	4.3(2)
C(2)	0.2913(5)	0.0781(5)	0.0964(3)	3.8(2)
C(3)	0.2960(5)	0.1044(5)	0.0350(4)	4.4(2)
C(4)	0.2876(6)	0.0481(6)	−0.0133(4)	4.8(2)
C(5)	0.2752(5)	−0.0047(5)	0.1086(4)	4.5(2)
C(6)	0.2674(6)	−0.0603(6)	0.0606(4)	5.3(2)
C(7)	0.2720(5)	−0.0330(6)	−0.0005(4)	4.4(2)
C(8)	0.2616(7)	−0.0947(6)	−0.0535(4)	6.7(3)
C(9)	0.3826(5)	0.1205(5)	0.2924(3)	4.1(2)
C(10)	0.3518(6)	0.0832(5)	0.3436(4)	5.1(2)
C(11)	0.4054(6)	0.0488(6)	0.3853(4)	5.4(2)
C(12)	0.4654(6)	0.1280(6)	0.2839(4)	5.2(2)
C(13)	0.5196(6)	0.0947(6)	0.3268(4)	5.7(2)
C(14)	0.4892(5)	0.0521(5)	0.3770(4)	4.5(2)
C(15)	0.5488(6)	0.0129(6)	0.4206(4)	6.4(3)
C(16)	0.215(2)	0.719(2)	0.296(2)	21(2)*
C(17)	0.2141(9)	0.631(2)	0.271(2)	16(1)*
C(18)	0.125	0.625	0.250	12.1(7)*

[a] Starred values indicate that atoms were refined isotropically. Anisotropically refined atoms are given in the form of the equivalent isotropic displacement parameter defined as $^1/_3[a^2B_{11} + b^2B_{22} + c^2B_{33} + 2ab(\cos\gamma)abB_{12} + 2ac(\cos\beta)acB_{13} + 2bc(\cos\alpha)bcB_{23}$.

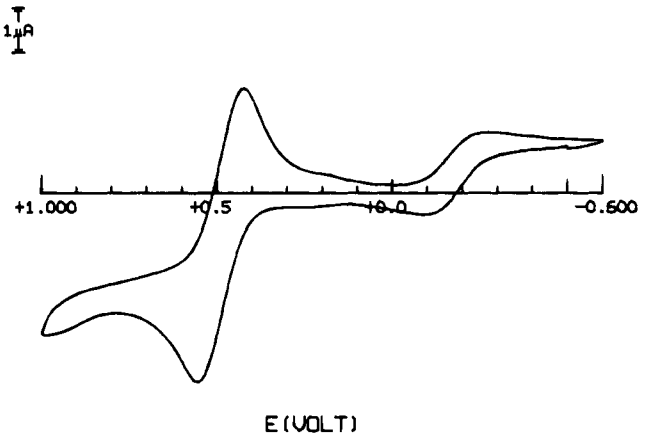

Figure 1. Cyclic voltammogram of $Ru_2(DtolF)_4Cl$ recorded in CH_2Cl_2 (scan rate: 100 mV/s).

The redox behavior of **1** is shown in the cyclic voltammogram, Figure 1. The oxidation wave at +495 mV (*vs* Ag/AgCl) indicates that a $Ru_2(DtolF)_4{}^{2+}$ species should be obtainable on a preparative scale. This result merits comparison with the recently reported[11] preparation of the compound $Ru_2(DPhF)_4(CCPh)_2$. The reason for the apparent non- or semireversible character of the reduction at −195 mV is not known. Further study of the electrochemistry of $Ru_2(DtolF)_4$ and $Ru_2(DtolF)_4Cl$, with proper attention to the influence of Cl^- concentration, would undoubtedly be worthwhile.

The molecular structure of $Ru_2(DtolF)_4Cl$ is shown in Figure 2, and selected bond distances and angles are listed in Table 3. As expected, the structure is qualitatively very similar to that of $Ru_2(DtolF)_4$, but with two important exceptions. First, and most important, the Ru−Ru distance is 2.370(2) Å, which is roughly 0.10 Å shorter than that in $Ru_2(DtolF)_4$, where it is

(7) North, A. C. T.; Phillips, D. C.; Mathews, F. S. *Acta Crystallogr., Sect. A: Cryst. Phys., Diffr., Theor. Gen. Crystallogr.* **1968**, *24A*, 351.
(8) Cotton, F. A.; Ren, T.; Eglin, J. L. *J. Am. Chem. Soc.* **1990**, *112*, 3439.
(9) Cotton, F. A.; Ren, T.; Eglin, J. L. *Inorg. Chem.* **1991**, *30*, 2552.
(10) Cotton, F. A.; Ren, T.; Eglin, J. L. *Inorg. Chem.* **1991**, *30*, 2559.
(11) Bear, J. L.; Han, B.; Huang, S. *J. Am. Chem. Soc.* **1993**, *115*, 1175.

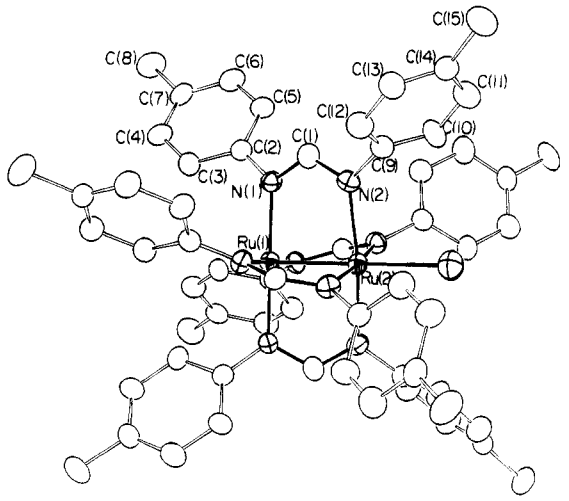

Figure 2. ORTEP view of $Ru_2(DtolF)_4Cl$.

Table 3. Selected Bond Distances (Å) and Angles (deg) for $Ru_2(DtolF)_4Cl{\cdot}C_6H_{14}$[a]

	Distances		
Ru(1)–Ru(2)	2.370(2)	Ru(2)–N(2)	2.092(7)
Ru(1)–N(1)	2.030(6)	N(1)–C(1)	1.33(1)
Ru(2)–Cl	2.412(5)	N(2)–C(1)	1.31(1)
	Angles		
Ru(2)–Ru(1)–N(1)	89.9(2)	Ru(2)–N(2)–C(1)	118.9(5)
Ru(1)–Ru(2)–N(2)	86.7(2)	N(1)–C(1)–N(2)	122.3(8)
Ru(1)–N(1)–C(1)	117.9(5)		

[a] Numbers in parentheses are estimated standard deviations in the least significant digits.

2.475(1) Å. The $Ru_2(DtolF)_4Cl$ molecule lies on a crystallographic C_4 axis, which is coincident with the Ru–Ru–Cl chain of atoms. This allows for a torsion angle about the Ru–Ru bond and there is, in fact, a torsion angle of 15.2(3)°, which is larger than that previously found in $Ru_2(DtolF)_4$, namely, about 9.5°. As we shall show below, both of these main differences between the $Ru_2(DtolF)_4$ and $Ru_2(DtolF)_4Cl$ structures are understandable in terms of the electronic structures of the two molecules.

Direct information concerning the electronic structure of $Ru_2(DtolF)_4Cl$ has been obtained from measurements of its magnetic susceptibility. The magnetic susceptibility data, together with fitted curves, are shown in Figure 3. The compound has an effective magnetic moment (μ_{eff}) of 3.66 μ_B at 300 K, which is consistent with a ground state having $S = {}^3/_2$. Moreover, the temperature dependences of χ and μ_{eff} closely resemble the dependences previously observed for $Ru_2(O_2CR)_4Cl$ compounds.[12,13] In these cases, it was shown that the moderate decrease in μ_{eff} at lower temperatures can be attributed to zero-field splitting (ZFS). In the present case, if we assume that $g_\perp = g_\parallel = 2.00$, the effective moment can be expressed as[14]

$$\mu_{eff} = \left(\frac{3kT}{N}\chi_{av}\right)^{1/2} = \left(\frac{3kT}{N}\frac{1}{3}(2\chi_\perp + \chi_\parallel)\right)^{1/2} = \left(9 + \frac{6}{x}\tanh x\right)^{1/2}\mu_B \quad (2)$$

where $x = D/kT$ and D is the ZFS parameter. Least-squares fitting of the measured μ_{eff} data to this equation yields a D value of 49.5(1.8) cm^{-1}, which is similar to the value obtained for $Ru_2(O_2CR)_4Cl$.[12,13] As shown in Figure 3, the consistency

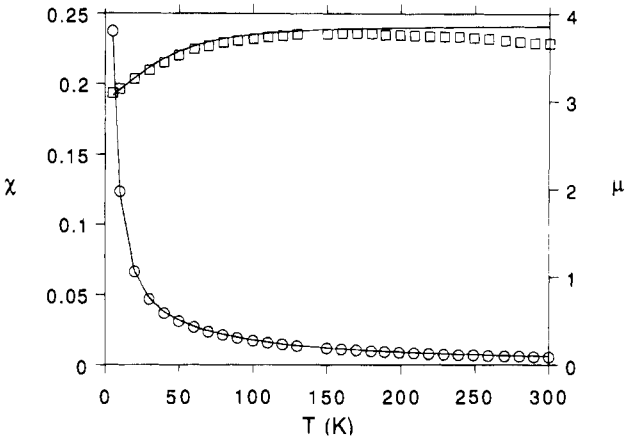

Figure 3. Measured magnetic susceptibility χ ($\times 10^{-3}$ emu; circles) and effective magnetic moment μ_{eff} (Bohr magneton, μ_B; squares) *vs* T (K) for $Ru_2(DtolF)_4Cl$. The solid line overlapped with the squares is the theoretical fit of μ_{eff} according to eq 2. The solid line overlapped with the circles is the susceptibility calculated from the theoretical fit of μ_{eff}.

Scheme 1

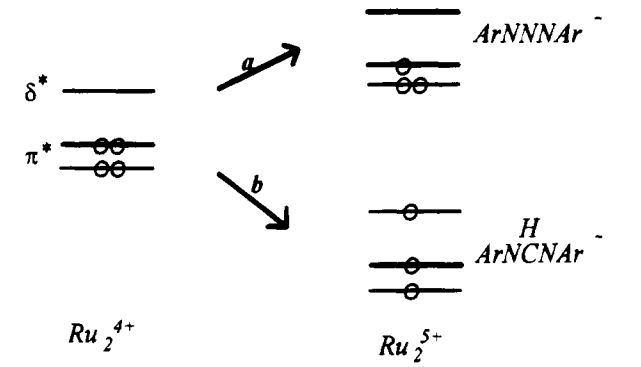

between the experiment and theory is clear for $T < 200$ K. The small discrepancy at higher temperatures is probably due to the isotropic character of the fitting model.

Similarly to the isoelectronic species $Ru_2(O_2CR)_4Cl$,[15] $Ru_2(DtolF)_4Cl$ displays two low-energy absorptions (λ_{max} (nm) 679 and 469), which are probably associated with the π^* to σ^* and δ^* to σ^* transitions. It is noteworthy that the transitions are much more intense than those observed for the carboxylates. This reflects the significant nitrogen contribution to the Ru–Ru (anti)bonding orbitals, which can be attributed to the strong basicity of DtolF.

Summary and Conclusions

The present work illustrates, once again, and in a very clear fashion, that the pattern of antibonding orbitals, δ^* and π^*, for multiply-bonded M_2^{n+} units is quite variable depending on the way in which these orbitals interact with orbitals on the ligands. It would appear that with the $ArNNNAr^-$ ligands the δ^* orbital is raised far enough above the π^* orbitals in both the Ru_2^{4+} and Ru_2^{5+} cores that they must remain empty in the ground states at room temperature. Thus, the result of converting $Ru_2(ArNNNAr)_4$ to $Ru_2(ArNNNAr)_4^+$ is that shown in Scheme 1 by the arrow **a**. The π^* to δ^* gap is large enough, even in the $Ru_2(ArNNNAr)_4^+$ case to make a $\pi^{*2}\delta^*$ configuration inaccessible. It may be, however, that the gap is only just large enough to lead to this result. We might expect the gap to be smaller when $ArNNNAr^-$ ligands are replaced by $ArNC(H)NAr^-$

(12) Cotton, F. A.; Pedersen, E. *Inorg. Chem.* **1979**, *18*, 388.
(13) Telser, J.; Drago, R. S. *Inorg. Chem.* **1984**, *23*, 3114.
(14) Carlin, R. L. *Magnetochemistry*; Springer-Verlag: Berlin, 1986.
(15) Miskowski, V. M.; Gray, H. B. *Inorg. Chem.* **1988**, *27*, 2501.

ligands. While it is, apparently, still large enough to maintain the π^{*4} configuration in $Ru_2(DtolF)_4$, it is not sufficient for the $Ru_2(DtolF)_4Cl$ molecule, and thus, in Scheme 1, oxidation follows the course indicated by arrow **b**.

Given that the change in electron configuration is from π^{*4} to $\pi^{*2}\delta^*$, the large decrease of *ca.* 0.10 Å in the Ru−Ru distance is fully understandable. While the loss of one π^* electron in the $Ru_2(ArNNNAr)_4^+$ compounds did not have much net influence on the Ru−Ru bond distance because the two opposing factors (vide supra) could approximately or nearly cancel its effect, the loss of a second π^* electron then exercises its full effect of 0.05−0.10 Å. It must be recognized that the effect of an electron in a δ^* orbital, which is only very weakly antibonding, is not at all comparable to the effect of a strongly antibonding π^* electron.

Acknowledgment. We thank the National Science Foundation for support. We also acknowledge Ms. D. Arnold for the measurement of the extinction coefficients and Prof. T. Datta and Dr. J. Amirzadek for the magnetic measurements.

Supplementary Material Available: Complete tables of crystal data, bond distance and angles, anisotropic displacement parameters, and the measured magnetic susceptibility of **1** between 5 and 300 K (7 pages). Ordering information is given on any current masthead page.

IC941365L